Evaluation of the GROMOS 56ACARBO Force Field for the Calculation of Structural, Volumetric and Dynamic Properties of Aqueous Glucose Systems

ARTICLE *in* THE JOURNAL OF PHYSICAL CHEMISTRY B · NOVEMBER 2015

Impact Factor: 3.3 · DOI: 10.1021/acs.jpcb.5b08155

THE JOURNAL OF PHYSICAL CHEMISTRY B

Article

pubs.acs.org/JPCB

Evaluation of the GROMOS 56A$_{CARBO}$ Force Field for the Calculation of Structural, Volumetric, and Dynamic Properties of Aqueous Glucose Systems

Marta L. S. Batista,[†,‡] Germán Pérez-Sánchez,[†] José R. B. Gomes,[†] João A. P. Coutinho,[†] and Edward J. Maginn*[,‡]

[†]Departamento de Química, CICECO, Universidade de Aveiro, Campus Universitário de Santiago, 3810-193 Aveiro, Portugal

[‡]Department of Chemical and Biomolecular Engineering, 182 Fitzpatrick Hall, University of Notre Dame, Notre Dame, Indiana 46556, United States

Supporting Information

ABSTRACT: Glucose is an important carbohydrate, relevant both for its biological functions and as a raw material for industrial processes. As a monomer of cellulose, the most abundant biopolymer, it is an alternative feedstock for fuels and chemicals in the biorefinery framework. Since glucose is often used and processed in aqueous solutions, it is important to understand the structural, volumetric, and dynamic properties of aqueous glucose solutions at varying concentrations. Molecular dynamics (MD) simulations are an effective means for computing the properties of liquid solutions, but the technique relies upon accurate intermolecular potential functions (i.e., "force fields"). Here we evaluate the accuracy of the recently developed GROMOS 56A$_{CARBO}$ glucose force field for its ability to model the density, viscosity, and self-diffusivity of aqueous glucose solutions as a function of concentration. We also compute different structural properties, including hydrogen bonds, radial and spatial distribution functions, and coordination numbers. The results show that the force field accurately models the density and viscosity of dilute solutions up to a glucose mole fraction of 0.1. At higher glucose concentrations, the force field overestimates the experimental density and viscosity. By analyzing the liquid structure, it is found that the glucose molecules tend to associate at higher concentrations, which leads to deviation from the experimental results. This suggests that, while the GROMOS 56A$_{CARBO}$ force field performs well for highly dilute glucose solutions (conditions under which it was developed), it is not appropriate for carrying out simulations of more concentrated glucose solutions. It is possible to obtain much more accurate densities and viscosities at high glucose concentrations by uniformly reducing the partial charges on glucose by 20%, which attenuates the self-association tendencies of glucose.

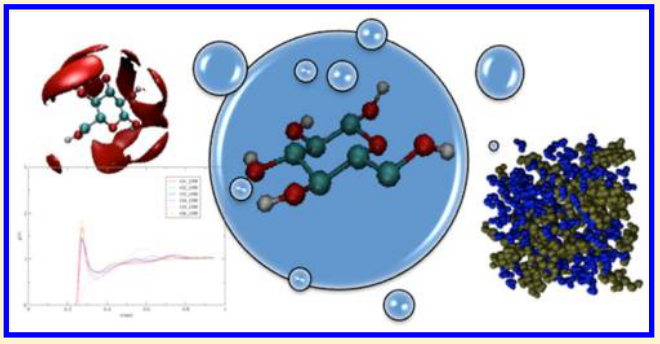

1. INTRODUCTION

Carbohydrates are an important and diverse class of biomolecules, characterized by a vast heterogeneity of compounds differing in their stereochemistry and functionalization. These compounds are essential to many biological functions and are also important in a wide range of industries including textile, food, pulp and paper, biofuels, and personal care.[1−3]

One particularly important carbohydrate is D-glucose, a hexopyranose with two stereoisomers, namely, α-D-glucopyranose and β-D-glucopyranose, with the latter being the dominant isomer in aqueous solution, in a proportion of 36:64.[4] Glucose is the monomer of cellulose, the most abundant biopolymer, which is being considered as a feedstock for the renewable production of fuels and chemicals.[1−3,5,6] Most biological and industrial processes involving glucose are carried out in aqueous media, so it is important to understand the structural, volumetric, and dynamic properties of aqueous glucose solutions. The most common experimental technique used to study the crystalline structure of glucose is X-ray diffraction, while techniques such as NMR and IR are commonly used to characterize aqueous solutions.[1−3] To help in the interpretation of the spectroscopic data, atomistic-level molecular dynamics (MD) simulations have also been performed, providing further understanding of the molecular interactions that occur in these systems.[2] MD simulations can also be used to predict macroscopic transport and thermodynamic properties of liquids.

A key requirement for these simulations is an accurate description of the inter- and intramolecular interactions, which are treated using a classical potential energy expression or "force field" (FF).[7] Several FFs have been developed for

Received: August 21, 2015
Revised: November 13, 2015

DOI: 10.1021/acs.jpcb.5b08155
J. Phys. Chem. B XXXX, XXX, XXX−XXX

carbohydrates, including OPLS,[8,9] AMBER,[10,11] CHARMM,[12,13] GLYCAM,[14,15] and GROMOS.[16,17] Within these, some were optimized and validated for hexopyranoses or systems composed of glucose.[18−21] For carbohydrates in aqueous solution, the different FFs have utilized different models for water and have been developed to capture different physical phenomena.[1,2] One of the most difficult features for a FF to capture for aqueous glucose solutions is epimerization or anomerization, i.e., the interconversion between the α-D-glucoyranose and β-D-glucopyranose (also called mutarotation). This phenomenon and other structural transitions occur due to a complex interplay between the electrostatic, steric, hydrogen bonding, and solvation effects present in the system, which is a difficult task for FFs to adequately reproduce and to take into account. Additionally, many of these processes occur over time scales that are long compared to MD simulation times, making their observation difficult without extremely long simulations.[1−3]

One of the key interactions between glucose and water are hydrogen bonds (H-bonds), which occur via the hydroxyl groups of glucose. The establishment of H-bonds is affected by the orientation of each hydroxyl and hydroxymethyl group in glucose, which in turn is affected by the anomeric effect, 1−3-syn-diaxial repulsions and solvation effects, each of which affects the stability of a given conformer.[22,23] It is thus clear that the study of the orientation of the hydroxyl groups in glucose is key for understanding the interactions between glucose and water. For this reason, the orientation and angles of the hydroxymethyl group (O5−C5−C6−O6, see Figure 1) and also the free lactol group (C1−O1, Figure 1) are commonly studied to evaluate if a given solvent is able to favorably interact with glucose.[24]

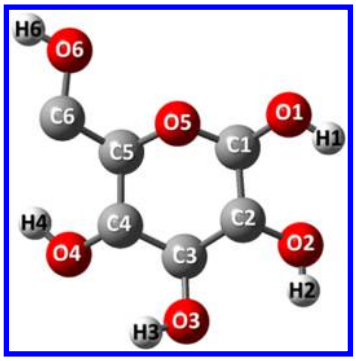

Figure 1. Atom labels used in this work for glucose. Color coding for spheres: red is O, gray is C, and white is H.

The newest version of the GROMOS carbohydrate FF, 56A$_{CARBO}$,[3] is adopted in this work to study the mechanisms of glucose and water interactions and the dynamical behavior of this system. This FF is an optimization of the GROMOS 53A6 FF,[25] and fixes a number of shortcomings, including the rotational preferences of the hydroxymethyl and free lactol groups. This was done by the introduction of specific Lennard-Jones interaction parameters to account for special intramolecular interactions that are specific for six-membered ring compounds and are responsible for the stability of conformations. The FF was validated by reproducing free energies of ring conformers, epimers, anomers, hydroxymethyl rotamers, and glycosidic linkages under dilute aqueous conditions.[3]

While the 56A$_{CARBO}$ force field appears to yield good dilute solution properties, we are interested in modeling aqueous glucose solutions at finite concentrations relevant to applications such as fermentation. Therefore, the objective of the present work is to test the accuracy of the GROMOS 56A$_{CARBO}$ force field at reproducing the volumetric, dynamic, and structural properties of aqueous glucose mixtures at finite concentrations. Six mixtures of β-D-glucopyranose and water at different concentrations were simulated using the GROMOS 56A$_{CARBO}$ FF for β-D-glucopyranose and the extended simple point charge (SPC/E) water model.[26] Densities, viscosities, and self-diffusivities were computed and compared with available experimental data. The structure of the solutions was examined by conducting a hydrogen bonding analysis and by computing radial and spatial distribution functions.

2. COMPUTATIONAL DETAILS

MD simulations were carried out for six systems composed of glucose and water using GROMACS version 4.5.5.[27] The systems contained 170 water molecules and 6, 9, 14, 20, 29, or 42 glucose molecules, yielding solutions with glucose mole fractions of 0.034, 0.050, 0.076, 0.105, 0.146, and 0.198, respectively. Each box was built with the PACKMOL package,[28] with a random distribution of the molecules and imposing a distance of 2.5 Å between atoms to ensure that no atomic overlapping occurs. Unless when clearly stated, water was modeled with the SPC/E FF,[26] and glucose was modeled with the GROMOS 56A$_{CARBO}$ FF.[3] The functional form of the glucose FF is given by

$$V = \sum_{ijk}^{N_\theta} \frac{1}{2} K_{\theta_{ijk}} [\cos(\theta_{ijk}) - \cos(\theta_{ijk})]^2 + \sum_{ijkl}^{N_\varphi} K_{\varphi_{ijkl}} [1 + \cos(m_\varphi \varphi_{ijkl} - \varphi_{0_{ijkl}})] + \sum_{ijkl}^{N_\xi} \frac{1}{2} K_{\xi_{ijk}} [\xi_{ijkl} - \xi_{0_{ijkl}}]^2 + \sum_{ij,j\neq i}^{LJ} \left[\frac{C_{ij}^{12}}{r_{ij}^{12}} - \frac{C_{ij}^{6}}{r_{ij}^{6}} \right] + \sum_{ij}^{c} \left[\frac{q_i q_j}{4\pi\varepsilon_0} \frac{1}{r_{ij}} \right] \quad (1)$$

where V is the total potential energy of the system and the symbols have their usual meaning.[29] Starting configurations were subjected to energy minimization followed by a 20 ns equilibration in the isothermal−isobaric (NpT) ensemble. During this period, the temperature was maintained at 313.15 K via a Nosé−Hoover thermostat[30,31] while the pressure was held at 1 bar with a Parrinello−Rahman barostat.[32] A cutoff of 0.9 nm was applied for nonbonded interactions, and corrections for long-range interactions were taken into account. The SHAKE algorithm was used to constrain all bonds, and a time step of 2 fs was considered in the simulations. The same procedure was performed for three independent configurations, and densities were estimated from the average of the three simulations.

Using the densities obtained from the NpT simulations, a configuration of the system at the average density for each considered mixture was taken and simulations were then run in the canonical (NVT) ensemble. The system was equilibrated by running an annealing schedule for 15 ns from 298.15 to 500.15 K and then finally to 313.15 K. Production runs were then

DOI: 10.1021/acs.jpcb.5b08155
J. Phys. Chem. B XXXX, XXX, XXX−XXX

carried out for an additional 65 ns (up to 105 ns in some simulations) at 313.15 K. A time step of 1 fs was utilized, with energies recorded every 10 fs. Once again, the SHAKE algorithm was employed to constrain all bonds, a cutoff of 0.9 nm was applied for nonbonded interactions, and corrections for long-range interactions were taken into account. Additionally, three independent NVT simulations of 20 ns duration were performed in order to estimate uncertainties. For these simulations, a time step of 2 fs was used. The independent trajectories were generated by assigning different initial velocity distributions to a given equilibrated configuration. All other conditions were the same as in the previous NVT runs.

While the simulations are long enough to determine structural and dynamic properties of a given stereoisomer, the interconversion between α-D-glucopyranose and β-D-glucopyranose requires longer time scales, and will thus not be observed during the MD simulations. Therefore, some caution is required when comparing computed and experimental results.

3. RESULTS AND DISCUSSION

3.1. Conformational Analysis. As previously mentioned, the study of the different angle conformations of specific groups can help infer the types of interactions that glucose is able to establish. The orientation of the hydroxymethyl moiety is impacted by the conformation of the dihedral angle (O5−C5−C6−O6, see Figure 1).[1,3] There are three known conformations for this dihedral angle: gauche−gauche (*gg*), where the angle is nominally −60°; trans−gauche (*tg*), with an angle of 180°; and gauche−trans (*gt*), with an angle of 60° (see Figure 2). This

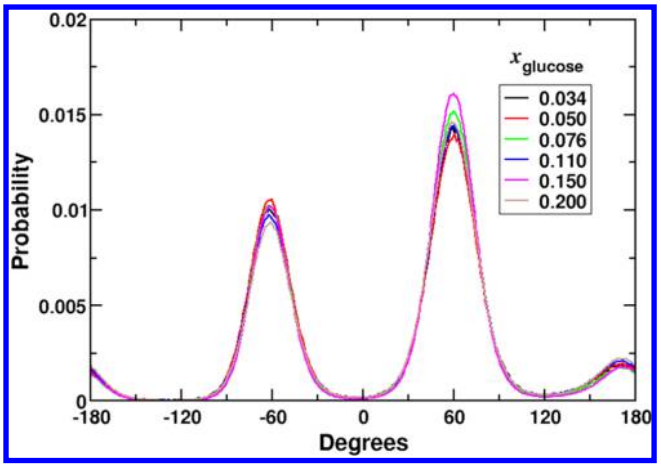

Figure 2. Probability distribution of the hydroxymethyl group angle in glucose as a function of concentration.

analysis was previously applied to a system composed of cellulose and water.[33] It is well-known that in the case of the crystalline structure of cellulose the *tg* conformation is predominant, while in aqueous solution the *gg* conformation becomes far more populated, followed by *gt* and *tg*.[34,35] For this reason, the conformation *tg* is associated with a crystalline-like state of glucose and the conformation *gg* is associated with an amorphous state of glucose in water. In the presence of other solvents, for example, ionic liquids, the *gt* conformation is the most populated state.[33,36]

The computed distribution of the hydroxymethyl group as a function of glucose concentration is shown in Figure 2. The results show that the predominant conformations are *gg* and *gt*, indicative of an amorphous structure for glucose when interacting with water. These results are similar for all six mixtures examined.

3.2. Density. Values of the densities for each mixture were used to evaluate the ability of the 56A$_{CARBO}$ force field for reproducing systems composed of glucose and water by comparison with experimental densities taken from Comesaña et al.[37] As can be seen in Figure 3, experimental and calculated

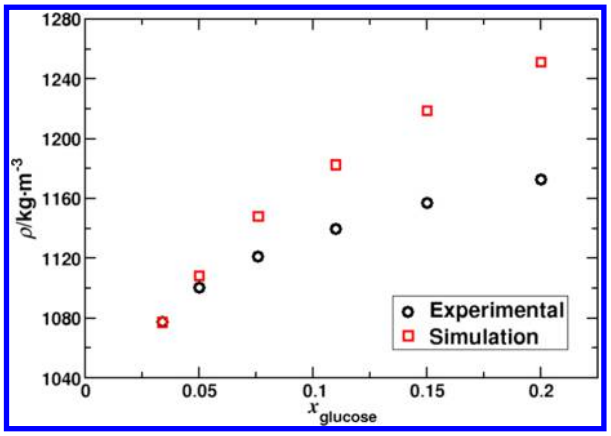

Figure 3. Comparison of experimental[37] and simulation density values at 313.15 K.

densities become larger with the increase of the glucose mole fraction in the mixtures. The calculated densities overestimate the experimental ones in the entire glucose mole fraction range considered in this work. Good agreement is found for the solution with the smallest glucose mole fraction (the difference is only 0.02%), but the difference reaches a maximum of 6.70% for 0.2 mole fraction (Table 1).

Table 1. Experimental[37] and Computational Densities (ρ) for Different Glucose/Water Mixtures at 313.15 K Modeled with the GROMOS 56A$_{CARBO}$ and SPC/E Force Fields, Respectively[a]

$x_{glucose}$	ρ_{exp} (kg·m^{-3})	ρ_{sim} (kg·m^{-3})	AAD[b] (%)
0.034	1077.6	1077.4 (±0.1)	0.02
0.050	1100.6	1108.4 (±0.1)	0.71
0.076	1121.2	1148.2 (±0.1)	2.41
0.110	1139.9	1182.6 (±0.4)	3.75
0.150	1157.1	1218.7 (±0.2)	5.32
0.200	1172.7	1251.3 (±0.5)	6.70

[a]Values in parentheses denote the uncertainties (the standard deviation) estimated with the calculated results. AAD represents the absolute deviations of the simulated data from the experimental values. [b]AAD = ABS($(\rho_{exp} - \rho_{sim})/\rho_{exp}$) × 100.

In order to understand if the consistent overestimation of the densities of the glucose aqueous solutions was due to deficiencies in the SPC/E or the 56A$_{CARBO}$ force fields, four new sets of MD simulations were executed using (i) the 56A$_{CARBO}$ force field for glucose and the TIP3P model[38] for water, (ii) the 56A$_{CARBO}$ force field for glucose and the SPC model[39] for water, (iii) the OPLS-AA[9] force field for glucose and the SPC/E model for water, and (iv) the OPLS-AA-SEI[8] force field for glucose and the SPC/E model for water. The TIP3P, SPC, and SPC/E water models are known to do a reasonable job in modeling pure water properties, with the latter being the most accurate for calculating the density and

DOI: 10.1021/acs.jpcb.5b08155
J. Phys. Chem. B XXXX, XXX, XXX−XXX

viscosity of water.[40] Calculated data are compared with experimental densities in Tables S1−S4 of the Supporting Information, which include also an analysis of the effects of the temperature and of the simulation box and cutoff sizes on the computed values. It is found that at low glucose concentrations all the models provide satisfactory results. At higher glucose concentrations, densities are always overestimated, but it is clear that the overestimations by the OPLS-AA (Table S3) and OPLS-AA-SEI (Table S4) force fields are larger than those found for the 56A$_{CARBO}$ model (Tables S1 and S2). This suggests that the water model is not the origin of the discrepancies between the experimental and calculated densities but that instead the problem lies in the glucose models (and the way they interact with water). These results highlight the limitations of currently available force fields for the description of glucose at finite concentrations. Despite the problems in matching experimental solution densities, other properties were computed to assess the overall performance of the glucose model.

3.3. Viscosity. Shear viscosity is an important transport property that can be determined from MD simulations via the following Green−Kubo relation

$$\eta = \frac{V}{k_B T}\int_0^\infty \langle P_{\alpha\beta}(t_0 + t)\cdot P_{\alpha\beta}(t_0)\rangle \, dt \quad (2)$$

where the brackets indicate an ensemble average, V is the volume of the system, T is the temperature, and k_B is the Boltzmann constant. Inside the brackets, $P_{\alpha\beta}$ are the off-diagonal components of the pressure tensor. To achieve good statistics, very long simulations are required. Numerical integration of eq 2 can lead to large errors, especially due to noise at long times. Following the work of Rey-Castro and Vega,[41] the numerical integral obtained via eq 2 was fit to a double exponential of the following form

$$\eta(t) = A\alpha\tau_1(1 - e^{-t/\tau_1}) + A(1 - \alpha)\tau_2(1 - e^{-t/\tau_2}) \quad (3)$$

where A and α are empirical fitting parameters, $0 < \alpha < 1$, and τ_1 and τ_2 are characteristic decay times that differ by an order of magnitude. These parameters were taken from a least-squares fit of eq 2 to the simulation results. The shear viscosity was estimated from eq 3 by taking the limit as t goes to infinity. The uncertainty $\Delta\eta$ was estimated via the following relation

$$\Delta\eta = \sqrt{\frac{2A[\alpha\tau_1 + (1 - \alpha)\tau_2]}{t_{max}}} \quad (4)$$

where t_{max} is the maximum decay time used in the computation of the autocorrelation function.[41] The values of the fitting parameters used in eq 3 are compiled in Table S5 of the Supporting Information, as a function of glucose mole fraction. Typical values of t_{max} ranged from 80 to 120 ns, depending on the viscosity of the solution. Viscosity results at a temperature of 313.15 K are depicted in Figure 4 together with the experimental values taken from Comesaña et al.[37] Figure 4 shows that simulated viscosities are significantly higher than the experimental data above a glucose mole fraction of 0.11. At lower glucose concentrations, agreement with experimental data is good, with a maximum deviation lower than 10% (see Table 2). This result is consistent with the density data, since overestimation of density should lead to slower dynamics and higher viscosities.

As with the densities, a comparison was made between the viscosities obtained from simulations using the 56A$_{CARBO}$ force field for glucose and the SPC/E (Table 2) or SPC (Table S6) water models, and also from simulations employing the SPC/E water model and the glucose OPLS-AA (Table S7) or OPLS-AA-SEI (Table S8) force fields. The results show that the OPLS-AA and OPLS-AA-SEI force fields also significantly overestimate the viscosity, especially in the case of OPLS-AA. In the case of the simulations combining the 56A$_{CARBO}$ and SPC force fields, the calculated viscosity values are systematically smaller than those calculated with the 56A$_{CARBO}$ and SPC/E combination, and for small glucose mole fractions, the viscosity is much smaller than the experimental value for pure water, which is in agreement with a previous study[40] where it is suggested that SPC/E is clearly better than SPC for reproducing the viscosity of liquid water.

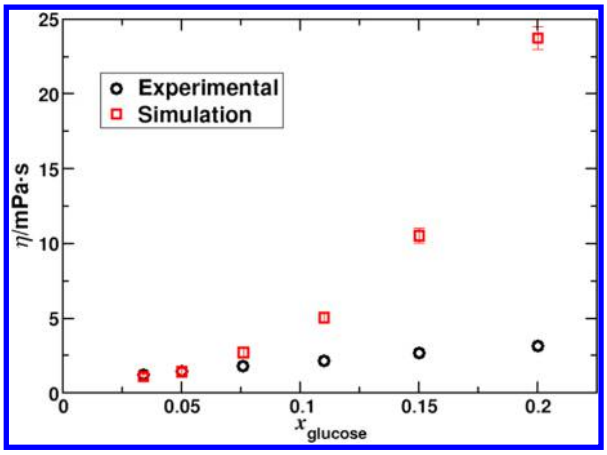

Figure 4. Comparison of experimental[37] and simulation viscosity values at 313.15 K. The standard deviations associated with the computed viscosities are also provided.

Table 2. Experimental[37] and Calculated Viscosities (η) for Different Glucose/Water Mixtures at 313.15 K Modeled with the GROMOS 56A$_{CARBO}$ and SPC/E Force Fields, Respectively[a]

$x_{glucose}$	η_{exp} (mPa·s)	η_{sim} (mPa·s)	AAD[b] (%)
0.034	1.205	1.129 (±0.168)	6.28
0.050	1.475	1.444 (±0.190)	2.12
0.076	1.804	2.722 (±0.262)	50.89
0.110	2.182	5.056 (±0.356)	131.70
0.150	2.660	10.556 (±0.514)	296.83
0.200	3.175	23.778 (±0.772)	648.90

[a]Values in parentheses denote uncertainties estimated according to eq 4. AAD represents the absolute deviations of the simulated data from the experimental values. [b]AAD = ABS$((\rho_{exp} - \rho_{sim})/\rho_{exp}) \times 100$.

3.4. Self-Diffusion Coefficients. Self-diffusion coefficients of water and glucose were computed via the following Einstein relation

$$D_i = \frac{1}{6}\lim_{t\to\infty}\frac{d}{dt}\langle[\overrightarrow{r_i(t)} - \overrightarrow{r_i(0)}]^2\rangle \quad (5)$$

where the term in brackets is the mean squared displacement. The slope of the mean squared displacement gives the value of D_i. In this work, slopes were determined over time intervals of 7500−10000 ps for glucose and 7500−12500 ps for water. The results are given in Table 3. As expected, water has a larger self-diffusion coefficient than glucose, and water mobility decreases with increasing glucose concentration. We are unaware of any experimental diffusivity data for the concentrations studied

DOI: 10.1021/acs.jpcb.5b08155
J. Phys. Chem. B XXXX, XXX, XXX−XXX

Table 3. Computed Self-Diffusion Coefficients for Different Glucose/Water Mixtures at 313.15 K Modeled with the GROMOS 56A$_{CARBO}$ and SPC/E Force Fields, Respectively[a]

$x_{glucose}$	D_{water} (1×10^{-5} cm^2/s)	$D_{glucose}$ (1×10^{-5} cm^2/s)
0.034	2.184 (±0.133)	0.346 (±0.021)
0.050	1.825 (±0.054)	0.280 (±0.009)
0.076	1.319 (±0.088)	0.217 (±0.007)
0.110	0.934 (±0.057)	0.088 (±0.012)
0.150	0.672 (±0.039)	0.085 (±0.001)
0.200	0.362 (±0.044)	0.035 (±0.010)

[a]Values in parentheses denote uncertainty (the standard deviation) associated with the calculated data.

here, but the simulation values are of the same magnitude as those measured experimentally by Ribeiro et al.[42] under different concentrations. Given the overestimation of the viscosities, we expect that the computed self-diffusivities are likely to be lower than the true values at higher glucose concentrations.

3.5. Radial Distributions Functions and Coordination Numbers. To probe the underlying structure of the solutions, radial distribution functions ($g(r)$ or RDF) were computed for various sites on glucose and water. Specifically, RDFs between glucose atoms O1, O2, O3, O4, O5, and O6 were computed with water OW atoms. In addition, water−water (OW−OW) and glucose−glucose (O1 with HO3, HO4, and HO6) RDFs were computed. Coordination numbers (CNs) for these pairs were obtained by integrating the RDFs out to a radial cutoff r_{CN}. This cutoff distance was, in all cases, the first local minimum of the corresponding RDF.

As mentioned previously, the mechanism of interaction between glucose and water is mediated through H-bonds. RDFs can provide information concerning the establishment of H-bonds in a mixture. According to geometric criteria, in the case of water−water interactions, a H-bond can be considered to exist when a site-to-site RDF O−O has a first minimum at a

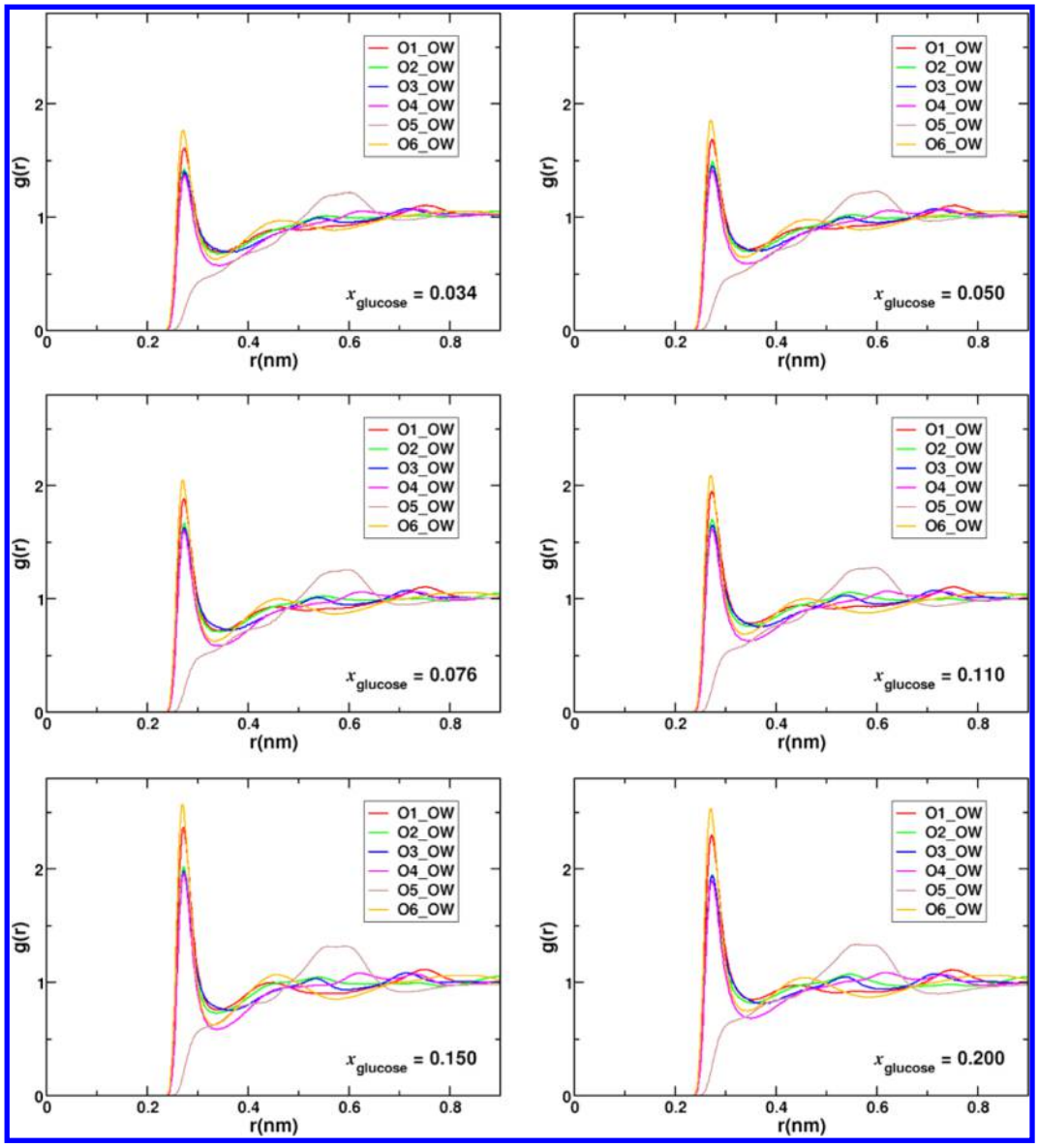

Figure 5. Radial distributions functions (RDFs) for O1−OW, O2−OW, O3−OW, O4−OW, O5−OW, and O6−OW glucose−water interactions, at six different glucose mole fractions ($x_{glucose}$) and a temperature of 313.15 K.

DOI: 10.1021/acs.jpcb.5b08155
J. Phys. Chem. B XXXX, XXX, XXX−XXX

distance less than 0.35 nm (or an O−H distance is less than 0.26 nm).[43] These values were used for r_{CN} to determine H-bonding interactions between glucose−water, glucose−glucose, and water−water. Results are shown in Figure 5 and also in Figures S1 and S2 of the Supporting Information.

It is possible to observe in Figure 5 that, with increasing glucose content, the heights of the peaks related with the water oxygen atoms surrounding the oxygen atoms of glucose increase. The peaks also become sharper, suggesting that the number of water molecules surrounding glucose is reduced and only a few strongly bound water molecules persist in the vicinity of glucose. This analysis is supported by the values of the coordination numbers, as discussed below. From the RDF heights, it can be understood that three types of atoms in glucose have an affinity toward water. Atoms O6 and O1 have the highest affinity for water, followed by atoms O2, O3, and O4. Atom O5 presents the lowest affinity for water, and from the RDF profile showing $g(r)$ values lower than 1, it is suggested that O5 is not establishing direct contacts with water molecules. This is presumably due to a steric hindrance effect. The results for atoms O6 and O1 agree with those reported in previous studies[22,23] where it was shown that these hydroxyl groups can interact with water as hydrogen bond acceptors. For water−water interactions, Figure S1 shows that the first water−water RDF peak becomes sharper as the concentration of glucose increases in the mixture. As is the case with the first peak in the water−glucose RDF, this is due to the fact that at high glucose concentrations water has only a few strongly associated neighboring water molecules.

Not surprisingly, glucose−glucose interactions increase with increasing concentrations of glucose. This can be seen in Figure S2, which shows various site−site RDFs for glucose−glucose interactions. The first peak occurs around 0.18 nm and is weak, with values of $g(r)$ below 1 at the lowest glucose concentration. As glucose concentration increases, this first peak approaches a value of 1.5. For all mixtures considered, the O1 atom of glucose interacts preferentially with HO6, which can be understood from a balance of steric effects.

The results for the coordination numbers are compiled in Table 4, as well as in Tables S9 and S10 of the Supporting Information. Confirming the observations made from the RDFs, there is a consistent decrease of the CN values for interactions between oxygen atoms in glucose and water oxygen atoms (OW) with increasing glucose concentration. Additionally, the CNs for O1−OW and O6−OW interactions are larger than those corresponding to the remaining glucose oxygen atoms. The CNs calculated for the water−water and glucose−glucose interactions, Tables S9 and S10, show a decrease in the water−water CNs and a slight increase in the glucose−glucose CNs with increasing glucose concentration.

The results suggest that, at low glucose content, glucose is interacting predominantly with water, and water with itself. As the number of glucose molecules increases in the system, glucose begins to self-associate. This self-association is likely overestimated in the simulations, which is why the density and transport properties do not agree with experiment at higher glucose concentrations. Improvements in the glucose force field will need to be made to modulate the degree of glucose self-association. Some strategies for doing this are outlined below.

3.6. Spatial Distribution Functions. Figure 6 shows three-dimensional spatial distribution functions (SDFs) for water about glucose. These plots were generated using the TRAVIS package.[44] Isosurfaces with values of 52 particle·nm^{-3} for oxygen atoms of water molecules are represented by the red surfaces around a central glucose molecule. Consistent with the RDFs and CNs, the SDFs show that, at low glucose concentrations, each glucose molecule is essentially surrounded by water. As the glucose concentration increases, other glucose molecules displace water, such that the glucose molecules are not completely solvated by water.

Table 4. Coordination Number (CN) from the RDF Peaks for Glucose−Water Interactions, at Each Mixture Considered

$x_{glucose}$	reference_atom	atom2	CN
0.034	O1	OW	2.54
	O2		2.33
	O3		2.38
	O4		2.13
	O5		
	O6		2.57
0.050	O1	OW	2.42
	O2		2.21
	O3		2.23
	O4		2.01
	O5		
	O6		2.42
0.076	O1	OW	2.21
	O2		2.03
	O3		2.07
	O4		1.85
	O5		
	O6		2.19
0.110	O1	OW	2.06
	O2		1.86
	O3		1.87
	O4		1.69
	O5		
	O6		2.01
0.150	O1	OW	1.82
	O2		1.62
	O3		1.66
	O4		1.48
	O5		
	O6		1.78
0.200	O1	OW	1.57
	O2		1.40
	O3		1.43
	O4		1.29
	O5		
	O6		1.57

3.7. Hydrogen Bonds. The definition of a hydrogen bond can be based on different criteria, but due to its simplicity, a geometric criterion is usually chosen, based on the distance between hydrogen and an acceptor (H−A) and the angle of H−O−A. The former is defined and chosen from the intermolecular site-to-site radial distribution functions, and the latter can be defined as 30° for intermolecular H-bonds and 60° for intramolecular H-bonds.[22] The definition for H-bonds established with water is that the distance of H−O is smaller than 0.26 nm (or the distance of O−O is smaller than 0.35 nm), and the angle H−O−O is smaller than 30°.[45,46] These are the criteria used in this work.

Figure 7 depicts the number of hydrogen bonds established between glucose and water per glucose molecule basis (red

DOI: 10.1021/acs.jpcb.5b08155
J. Phys. Chem. B XXXX, XXX, XXX−XXX

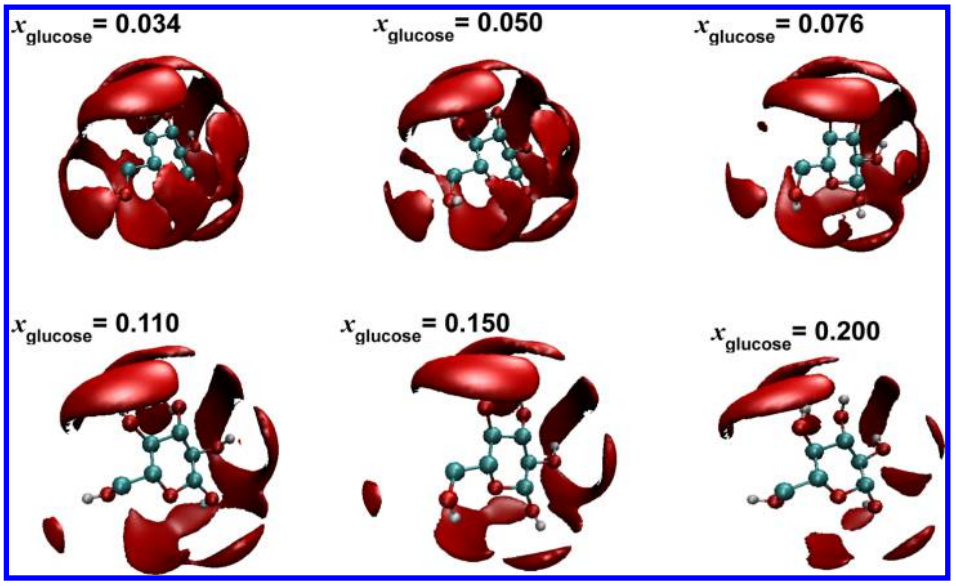

Figure 6. Variation of the spatial distribution functions (SDFs) with the glucose concentration. Red surfaces denote regions populated by oxygen atoms of the water molecules. Color coding for spheres: red is O, blue is C, and white is H.

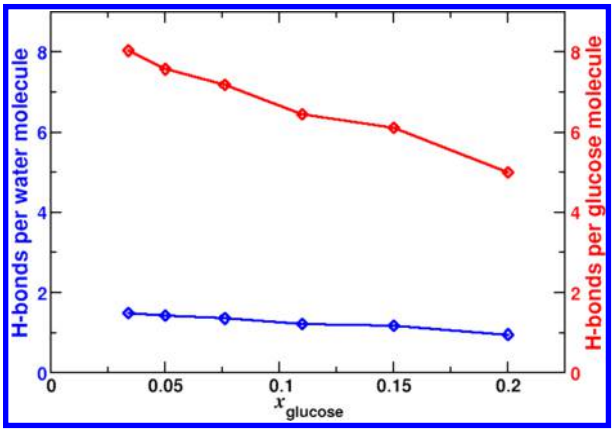

Figure 7. Number of hydrogen bonds between glucose and water molecules (red, right axis) and water with water molecules (blue, left axis) as a function of glucose concentration, at 313.15 K.

series) and between water molecules per water molecule basis (blue series). Numerical values are given in Table S11 of the Supporting Information. As expected, and in agreement with previous results, the number of H-bonds established between glucose and water decreases with increasing glucose concentration, as does the number of water−water H-bonds.

4. STRATEGY TO REFINE GLUCOSE FORCE FIELD FOR MIXTURES WITH WATER

Several works are found in the literature aiming at the improvement of force fields to reproduce properties of different systems, such as viscosity and diffusivity.[47−50] These improvements are often based on the usage of different strategies to estimate atomic partial charges (e.g., CHelpG,[51] Blöchl,[52] NPA[53,54]), or on the consideration of polarizable force fields with the introduction, for example, of Drude oscillators[55] (for ionic liquids, see Batista et al.[56]). The consideration of different approaches (e.g., CHelpG, NPA) for calculating the atomic charges leads to different sets of values. The magnitude of the charges is found to have a direct influence on the properties calculated for a specific system.[47,57,58] Thus, rescaling atomic charges has been found to be a simple way to improve the description of a system under study and to obtain properties that are in suitable agreement with the experimental ones (e.g., transport properties of systems composed of ionic liquids[57,59−61]).

Given that the current study found that the 56A$_{CARBO}$ FF tends to self-associate too strongly at finite concentrations, we hypothesized that the partial charges used in this model are too large and thus overpolarize glucose. We therefore tested whether uniformly scaling the partial charges on glucose by a factor less than unity would improve density and viscosity results at glucose mole fractions above ∼0.1. After testing different scaling factors between 1.00 and 0.75 using a step of 0.05, it was found that scaling all the partial charges on glucose by 0.8 gave much more reasonable results. Simulations using the rescaled charges, without changing the other simulation parameters, were repeated for systems with glucose mole fractions of 0.034, 0.050, 0.076, 0.110, 0.150, and 0.200. New density and viscosity values are depicted as green triangles in Figures 8 and 9, while Tables S12 and S13 contain the

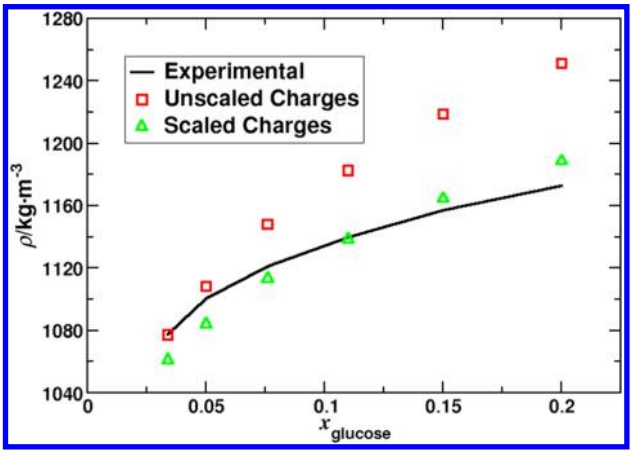

Figure 8. Comparison of experimental[37] (black curve) and simulation density values estimated with scaled charges (green triangles) and with the original charges (red squares) at 313.15 K.

DOI: 10.1021/acs.jpcb.5b08155
J. Phys. Chem. B XXXX, XXX, XXX−XXX

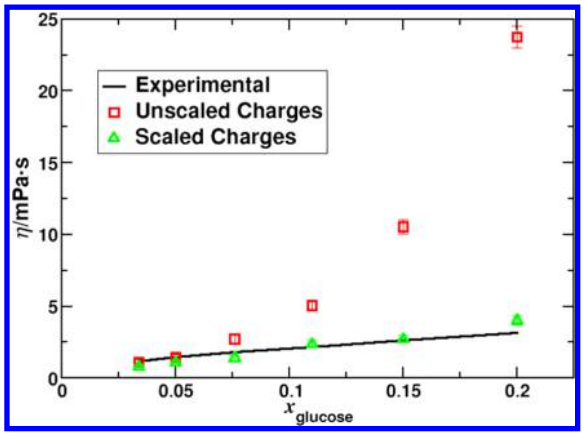

Figure 9. Comparison of experimental[37] (black curve) and simulation viscosity values estimated with scaled charges (green triangles) and with the original charges (red squares) at 313.15 K. The standard deviations associated with the computed viscosities are also provided.

numerical values. The experimental values (black curve) and previously predicted values (without rescaling charges, red squares) are also included in these figures. The scaled charge FF gives a maximum deviation of 1.6% for the density (versus 7% in the simulations with original glucose atomic charges) and of 35% for the viscosity (versus ~650% in the simulations with original glucose atomic charges). The improvement in these properties is significant, especially for the systems with a glucose mole fraction above 0.1. For systems with glucose mole fractions below 0.1, the scaled charge FF slightly underestimates both density and viscosity and performs slightly worse than the unscaled charge FF, but overall performance is good across all concentrations.

On the whole, the present results suggest that the rescaling charge methodology yields density and viscosity values in adequate agreement with experiment. A significant decrease in the deviations to the experimental data is found for both properties, but it is much more pronounced in the case of viscosity (Tables S12 and S13). However, this improvement was only attained where the GROMOS $56A_{CARBO}$ FF fails to predict density and viscosity values (i.e., at glucose mole fractions above 0.1). These results suggest that the use of polarizable force fields, such as that recently proposed by Patel et al.,[55] may be needed to obtain a high degree of accuracy across wide concentration ranges.

5. CONCLUSIONS

A molecular dynamics simulation study was carried out to determine the properties of aqueous solutions of D-glucose as a function of glucose concentration. The $56A_{CARBO}$ was selected to model glucose, and the SPC/E model was used for water. The glucose force field has been well tested under infinite dilution aqueous conditions but has not been evaluated for its ability to model properties under finite glucose concentrations. In the present work, densities, viscosities, and self-diffusivities were computed and compared to available experimental data. The structure of each solution was characterized via hydrogen bond analysis, coordination numbers, and radial and spatial distributions functions.

The computed densities and viscosities showed reasonable agreement with experiment below a glucose mole fraction of 0.15, but deviations became significant at higher concentrations. Specifically, computed densities were over 5% too large at high concentrations, while viscosities were overestimated by more than 100%. At the lowest concentrations studied (where the properties are dominated by water−water interactions), the densities and viscosities agreed well with experimental data. Some tests were run with alternative glucose force fields (OPLS-AA and OPLS-AA-SEI) and also with different water models (TIP3P and SPC). The OPLS force fields performed slightly worse than the $56A_{CARBO}$ force field at reproducing experimental densities and viscosities. Also, while small differences in the results for density and viscosity are observed when changing water force fields, system size, and cutoff distance, the overall results are consistent: the $56A_{CARBO}$ force field exhibits too strong an association tendency at high glucose concentrations, leading to an overestimation of the density and viscosity.

Self-diffusivities were also computed with the $56A_{CARBO}$ and SPC/E model force fields for glucose and water, respectively, and while there are no experimental data under the conditions of the simulations, it is expected that the simulated self-diffusivities are too low, given the trend with viscosity.

By examining hydrogen bond formation, coordination numbers, and spatial/radial distribution functions, it was determined that the glucose molecules tend to self-associate at finite concentrations. In essence, water does not fully hydrate the glucose molecules at higher concentrations, which leads to the overestimation of density and viscosity. The results suggest that improved glucose force fields could be developed if modifications are made to attenuate these self-interactions between glucose molecules and to promote better water solvation.

Preliminary studies utilizing a modified version of the $56A_{CARBO}$ force field for glucose, obtained by scaling the atomic charges of glucose by a factor of 0.8, and the SPC/E model for water, lead to significant improvements in the values of the calculated densities and viscosities at glucose mole fractions in the range from 0.034 to 0.200, without decreasing too much the quality of the results at diluted mole fractions.

■ ASSOCIATED CONTENT

Supporting Information

The Supporting Information is available free of charge on the ACS Publications website at DOI: 10.1021/acs.jpcb.5b08155.

Tables containing densities and viscosities for the mixtures of glucose−water, radial distribution functions, and coordination numbers for water−water and glucose−glucose interactions (PDF)

■ AUTHOR INFORMATION

Corresponding Author

*Phone: +1 574 631 5687. Fax: +1 574 631 8366. E-mail: ed@nd.edu.

Notes

The authors declare no competing financial interest.

■ ACKNOWLEDGMENTS

The authors thank Fundação para a Ciência e Tecnologia (FCT) for funding, for project PEst-C/CTM/LA0011/2013 and for Programa Investigador FCT. FCT is also recognized for the PhD grant SFRH/BD/74551/2010 of M.L.S.B. Thanks are due as well to the Center for Research Computing at the University of Notre Dame for providing access to computational resources. The authors acknowledge the help provided

DOI: 10.1021/acs.jpcb.5b08155
J. Phys. Chem. B XXXX, XXX, XXX−XXX

by Akash Sharma, who unfortunately passed away before this work was completed.

REFERENCES

(1) Fadda, E.; Woods, R. J. Molecular Simulations of Carbohydrates and Protein-Carbohydrate Interactions: Motivation, Issues and Prospects. *Drug Discovery Today* **2010**, *15*, 596−609.

(2) Foley, B. L.; Tessier, M. B.; Woods, R. J. Carbohydrate Force Fields. *Wiley Interdiscip. Rev. Comput. Mol. Sci.* **2012**, *2*, 652−697.

(3) Hansen, H. S.; Hünenberger, P. H. A Reoptimized GROMOS Force Field for Hexopyranose-Based Carbohydrates Accounting for the Relative Free Energies of Ring Conformers, Anomers, Epimers, Hydroxymethyl Rotamers, and Glycosidic Linkage Conformers. *J. Comput. Chem.* **2011**, *32*, 998−1032.

(4) Mason, P. E.; Neilson, G. W.; Enderby, J. E.; Saboungi, M.-L.; Brady, J. W. Structure of Aqueous Glucose Solutions as Determined by Neutron Diffraction with Isotopic Substitution Experiments and Molecular Dynamics Calculations. *J. Phys. Chem. B* **2005**, *109*, 13104−13111.

(5) Mayes, H. B.; Tian, J.; Nolte, M. W.; Shanks, B. H.; Beckham, G. T.; Gnanakaran, S.; Broadbelt, L. J. Sodium Ion Interactions with Aqueous Glucose: Insights from Quantum Mechanics, Molecular Dynamics, and Experiment. *J. Phys. Chem. B* **2014**, *118*, 1990−2000.

(6) Matthews, J. F.; Beckham, G. T.; Bergenstråhle-Wohlert, M.; Brady, J. W.; Himmel, M. E.; Crowley, M. F. Comparison of Cellulose Iβ Simulations with Three Carbohydrate Force Fields. *J. Chem. Theory Comput.* **2012**, *8*, 735−748.

(7) Gubbins, K. E.; Moore, J. D. Molecular Modeling of Matter: Impact and Prospects in Engineering. *Ind. Eng. Chem. Res.* **2010**, *49*, 3026−3046.

(8) Kony, D.; Damm, W.; Stoll, S.; Van Gunsteren, W. F. An Improved OPLS-AA Force Field for Carbohydrates. *J. Comput. Chem.* **2002**, *23*, 1416−1429.

(9) Damm, W.; Frontera, A.; Tirado-Rives, J.; Jorgensen, W. L. OPLS All-Atom Force Field for Carbohydrates. *J. Comput. Chem.* **1997**, *18*, 1955−1970.

(10) Glennon, T. M.; Zheng, Y.-J.; Le Grand, S. M.; Shutzberg, B. A.; Merz, K. M. A Force Field for Monosaccharides and (1 ? 4) Linked Polysaccharides. *J. Comput. Chem.* **1994**, *15*, 1019−1040.

(11) Momany, F. A.; Willett, J. L. Computational Studies on Carbohydrates: In Vacuo Studies Using a Revised AMBER Force Field, AMB99C, Designed for α-(1→4) Linkages. *Carbohydr. Res.* **2000**, *326*, 194−209.

(12) Ha, S. N.; Giammona, A.; Field, M.; Brady, J. W. A Revised Potential-Energy Surface for Molecular Mechanics Studies of Carbohydrates. *Carbohydr. Res.* **1988**, *180*, 207−221.

(13) Guvench, O.; Hatcher, E. R.; Venable, R. M.; Pastor, R. W.; Mackerell, A. D. CHARMM Additive All-Atom Force Field for Glycosidic Linkages between Hexopyranoses. *J. Chem. Theory Comput.* **2009**, *5*, 2353−2370.

(14) Woods, R. J.; Dwek, R. A.; Edge, C. J.; Fraser-Reid, B. Molecular Mechanical and Molecular Dynamic Simulations of Glycoproteins and Oligosaccharides. 1. GLYCAM_93 Parameter Development. *J. Phys. Chem.* **1995**, *99*, 3832−3846.

(15) Kirschner, K. N.; Yongye, A. B.; Tschampel, S. M.; González-Outeiriño, J.; Daniels, C. R.; Foley, B. L.; Woods, R. J. GLYCAM06: A Generalizable Biomolecular Force Field. Carbohydrates. *J. Comput. Chem.* **2008**, *29*, 622−655.

(16) Koehler, J. E. H.; Saenger, W.; Gunsteren, W. F. A Molecular Dynamics Simulation of Crystalline ?-Cyclodextrin Hexahydrate. *Eur. Biophys. J.* **1987**, *15*, 197−210.

(17) Lins, R. D.; Hünenberger, P. H. A New GROMOS Force Field for Hexopyranose-Based Carbohydrates. *J. Comput. Chem.* **2005**, *26*, 1400−1412.

(18) Lelong, G.; Howells, W. S.; Brady, J. W.; Talón, C.; Price, D. L.; Saboungi, M.-L. Translational and Rotational Dynamics of Monosaccharide Solutions. *J. Phys. Chem. B* **2009**, *113*, 13079−13085.

(19) Ziemys, A.; Ferrari, M.; Cavasotto, C. N. Molecular Modeling of Glucose Diffusivity in Silica Nanochannels. *J. Nanosci. Nanotechnol.* **2009**, *9*, 6349−6359.

(20) Biarnés, X.; Ardèvol, A.; Planas, A.; Rovira, C. Substrate Conformational Changes in Glycoside Hydrolase Catalysis. A First-Principles Molecular Dynamics Study. *Biocatal. Biotransform.* **2010**, *28*, 33.

(21) Zhang, J.; Zheng, Q.; Zhang, H. Unbinding of Glucose from Human Pulmonary Surfactant Protein D Studied by Steered Molecular Dynamics Simulations. *Chem. Phys. Lett.* **2010**, *484*, 338−343.

(22) Chen, C.; Li, W. Z.; Song, Y. C.; Weng, L. D.; Zhang, N. Formation of Water and Glucose Clusters by Hydrogen Bonds in Glucose Aqueous Solutions. *Comput. Theor. Chem.* **2012**, *984*, 85−92.

(23) Suzuki, T. The Hydration of Glucose: The Local Configurations in Sugar-Water Hydrogen Bonds. *Phys. Chem. Chem. Phys.* **2008**, *10*, 96−105.

(24) Chen, T.; Chidambaram, M.; Lin, Z. P.; Smit, B.; Bell, A. T. Viscosities of the Mixtures of 1-Ethyl-3-Methylimidazolium Chloride with Water, Acetonitrile and Glucose: A Molecular Dynamics Simulation and Experimental Study. *J. Phys. Chem. B* **2010**, *114*, 5790−5794.

(25) Oostenbrink, C.; Villa, A.; Mark, A. E.; van Gunsteren, W. F. A Biomolecular Force Field Based on the Free Enthalpy of Hydration and Solvation: The GROMOS Force-Field Parameter Sets 53A5 and 53A6. *J. Comput. Chem.* **2004**, *25*, 1656−1676.

(26) Berendsen, H. J. C.; Grigera, J. R.; Straatsma, T. P. The Missing Term in Effective Pair Potentials. *J. Phys. Chem.* **1987**, *91*, 6269−6271.

(27) Hess, B.; Kutzner, C.; van der Spoel, D.; Lindahl, E. GROMACS 4: Algorithms for Highly Efficient, Load-Balanced, and Scalable Molecular Simulation. *J. Chem. Theory Comput.* **2008**, *4*, 435−447.

(28) Martínez, L.; Andrade, R.; Birgin, E. G.; Martínez, J. M. PACKMOL: A Package for Building Initial Configurations for Molecular Dynamics Simulations. *J. Comput. Chem.* **2009**, *30*, 2157−2164.

(29) Allen, M. P.; Tildesley, D. J. *Computer Simulation of Liquids*; Oxford University Press: Oxford, U.K., 1989.

(30) Hoover, W. G. Canonical Dynamics - Equilibrium Phase-Space Distributions. *Phys. Rev. A: At., Mol., Opt. Phys.* **1985**, *31*, 1695−1697.

(31) Nose, S. A Molecular-Dynamics Method For Simulations in the Canonical Ensemble. *Mol. Phys.* **1984**, *52*, 255−268.

(32) Parrinello, M.; Rahman, A. Polymorphic Transitions in Single-Crystals - A New Molecular-Dynamics Method. *J. Appl. Phys.* **1981**, *52*, 7182−7190.

(33) Liu, H.; Sale, K. L.; Holmes, B. M.; Simmons, B. A.; Singh, S. Understanding the Interactions of Cellulose with Ionic Liquids: A Molecular Dynamics Study. *J. Phys. Chem. B* **2010**, *114*, 4293−4301.

(34) Nishiyama, Y.; Langan, P.; Chanzy, H. Crystal Structure and Hydrogen-Bonding System in Cellulose Iβ from Synchrotron X-Ray and Neutron Fiber Diffraction. *J. Am. Chem. Soc.* **2002**, *124*, 9074−9082.

(35) Nishiyama, Y.; Sugiyama, J.; Chanzy, H.; Langan, P. Crystal Structure and Hydrogen Bonding System in Cellulose I(alpha) from Synchrotron X-Ray and Neutron Fiber Diffraction. *J. Am. Chem. Soc.* **2003**, *125*, 14300−14306.

(36) Liu, H.; Cheng, G.; Kent, M.; Stavila, V.; Simmons, B. A.; Sale, K. L.; Singh, S. Simulations Reveal Conformational Changes of Methylhydroxyl Groups during Dissolution of Cellulose Iβ in Ionic Liquid 1-Ethyl-3-Methylimidazolium Acetate. *J. Phys. Chem. B* **2012**, *116*, 8131−8138.

(37) Comesaña, J. F.; Otero, J. J.; García, E.; Correa, A. Densities and Viscosities of Ternary Systems of Water + Glucose + Sodium Chloride at Several Temperatures. *J. Chem. Eng. Data* **2003**, *48*, 362−366.

(38) Jorgensen, W. L.; Chandrasekhar, J.; Madura, J. D.; Impey, R. W.; Klein, M. L. Comparison of Simple Potential Functions for Simulating Liquid Water. *J. Chem. Phys.* **1983**, *79*, 926.

(39) Berendsen, H. J. C.; Postma, J. P. M.; van Gunsteren, W. F.; Hermans, J. Interaction Models for Water in Relation to Protein Hydration. In The Jerusalem Symposia on Quantum Chemistry and

DOI: 10.1021/acs.jpcb.5b08155
J. Phys. Chem. B XXXX, XXX, XXX−XXX

Biochemistry; Pullman, B., Ed.; Springer: Dordrecht, The Netherlands, 1981; Vol. *14*, pp 331−342.
(40) Song, Y.; Dai, L. L. The Shear Viscosities of Common Water Models by Non-Equilibrium Molecular Dynamics Simulations. *Mol. Simul.* **2010**, *36*, 560−567.
(41) Rey-Castro, C.; Vega, L. F. Transport Properties of the Ionic Liquid 1-Ethyl-3-Methylimidazolium Chloride from Equilibrium Molecular Dynamics Simulation. The Effect of Temperature. *J. Phys. Chem. B* **2006**, *110*, 14426−14435.
(42) Ribeiro, A. C. F.; Ortona, O.; Simões, S. M. N.; Santos, C. I. A. V.; Prazeres, P. M. R. A.; Valente, A. J. M.; Lobo, V. M. M.; Burrows, H. D. Binary Mutual Diffusion Coefficients of Aqueous Solutions of Sucrose, Lactose, Glucose, and Fructose in the Temperature Range from (298.15 to 328.15) K. *J. Chem. Eng. Data* **2006**, *51*, 1836−1840.
(43) Skarmoutsos, I.; Dellis, D.; Matthews, R. P.; Welton, T.; Hunt, P. A. Hydrogen Bonding in 1-Butyl- and 1-Ethyl-3-Methylimidazolium Chloride Ionic Liquids. *J. Phys. Chem. B* **2012**, *116*, 4921−4933.
(44) Brehm, M.; Kirchner, B. TRAVIS - a Free Analyzer and Visualizer for Monte Carlo and Molecular Dynamics Trajectories. *J. Chem. Inf. Model.* **2011**, *51*, 2007−2023.
(45) Luzar, A.; Chandler, D. Hydrogen-Bond Kinetics in Liquid Water. *Nature* **1996**, *379*, 55−57.
(46) Haughney, M.; Ferrario, M.; McDonald, I. R. Pair Interactions and Hydrogen-Bond Networks in Models of Liquid Methanol. *Mol. Phys.* **1986**, *58*, 849−853.
(47) Youngs, T. G. A.; Hardacre, C. Application of Static Charge Transfer within an Ionic-Liquid Force Field and Its Effect on Structure and Dynamics. *ChemPhysChem* **2008**, *9*, 1548−1558.
(48) Dommert, F.; Wendler, K.; Berger, R.; Delle Site, L.; Holm, C. Force Fields for Studying the Structure and Dynamics of Ionic Liquids: A Critical Review of Recent Developments. *ChemPhysChem* **2012**, *13*, 1625−1637.
(49) Schröder, C. Comparing Reduced Partial Charge Models with Polarizable Simulations of Ionic Liquids. *Phys. Chem. Chem. Phys.* **2012**, *14*, 3089.
(50) Kirchner, B. In *Topics in Current Chemistry*; Balzani, V., De Meijere, A., Houk, K. N., Kessler, H., Lehn, J.-M., Ley, S. V., Olivucci, M., Schreiber, S., Thiem, J., Trost, B. M., Vogel, P., Vögtle, F., Wong, H., Yamamoto, H., Eds.; Springer: Berlin, Germany, 2009.
(51) Breneman, C. M.; Wiberg, K. B. Determining Atom-Centered Monopoles from Molecular Electrostatic Potentials. The Need for High Sampling Density in Formamide Conformational Analysis. *J. Comput. Chem.* **1990**, *11*, 361−373.
(52) Blöchl, P. E. Electrostatic Decoupling of Periodic Images of Plane-Wave-Expanded Densities and Derived Atomic Point Charges. *J. Chem. Phys.* **1995**, *103*, 7422.
(53) Reed, A. E.; Curtiss, L. A.; Weinhold, F. Intermolecular Interactions from a Natural Bond Orbital, Donor-Acceptor Viewpoint. *Chem. Rev.* **1988**, *88*, 899−926.
(54) Reed, A. E.; Weinstock, R. B.; Weinhold, F. Natural Population Analysisa). *J. Chem. Phys.* **1985**, *83*, 735.
(55) Patel, D. S.; He, X.; MacKerell, A. D. Polarizable Empirical Force Field for Hexopyranose Monosaccharides Based on the Classical Drude Oscillator. *J. Phys. Chem. B* **2015**, *119*, 637−652.
(56) Batista, M. L. S.; Coutinho, J. A. P.; Gomes, J. R. B. Prediction of Ionic Liquids Properties through Molecular Dynamics Simulations | BenthamScience. *Curr. Phys. Chem.* **2014**, *4*, 151−172.
(57) Ghatee, M. H.; Zolghadr, A. R.; Moosavi, F.; Ansari, Y. Studies of Structural, Dynamical, and Interfacial Properties of 1-Alkyl-3-Methylimidazolium Iodide Ionic Liquids by Molecular Dynamics Simulation. *J. Chem. Phys.* **2012**, *136*, 124706.
(58) Zhang, Y.; Maginn, E. J. A Simple AIMD Approach to Derive Atomic Charges for Condensed Phase Simulation of Ionic Liquids. *J. Phys. Chem. B* **2012**, *116*, 10036−10048.
(59) Bhargava, B. L.; Balasubramanian, S. Refined Potential Model for Atomistic Simulations of Ionic Liquid [bmim][PF6]. *J. Chem. Phys.* **2007**, *127*, 114510.
(60) Chaban, V. Polarizability versus Mobility: Atomistic Force Field for Ionic Liquids. *Phys. Chem. Chem. Phys.* **2011**, *13*, 16055−16062.
(61) Dommert, F.; Schmidt, J.; Krekeler, C.; Zhao, Y. Y.; Berger, R.; Delle Site, L.; Holm, C. Towards Multiscale Modeling of Ionic Liquids: From Electronic Structure to Bulk Properties. *J. Mol. Liq.* **2010**, *152*, 2−8.

DOI: 10.1021/acs.jpcb.5b08155
J. Phys. Chem. B XXXX, XXX, XXX−XXX